2015

# Research progress on design strategies, synthesis and performance of LiMn2O4-based cathodes

Fangxin Mao
*Hunan University*

Wei Dong Guo
*Anyang Normal University*, wdguo@uow.edu.au

Jianmin Ma
*University of Wollongong*

## Publication Details

Mao, F., Guo, W. & Ma, J. (2015). Research progress on design strategies, synthesis and performance of LiMn2O4-based cathodes. RSC Advances: an international journal to further the chemical sciences, 5 (127), 105248-105258.

# Research progress on design strategies, synthesis and performance of LiMn2O4-based cathodes

**Abstract**
Spinel LiMn2O4 (LMO)-based composites, due to their combination of low toxicity, abundant natural resources, and excellent electrochemical performance, are regarded as promising candidate cathode materials for lithium ion batteries. Current energy storage demands are not being met with existing materials, however, because of their defects, such as fast capacity fading, low rate capability, and low specific capacity in practical applications. Manganese dissolution during electrochemical processes bears the major responsibility for capacity loss, apart from the electrolyte factor. Low electrical conductivity, low ionic diffusion efficiency, and large structural variation have adverse effects on the electrochemical performance of materials. With respect to these drawbacks, significant progress has been made recently on optimizing the performance of LMO-based cathode materials. In this work, we review recent progress in 1 structural design, designing composites with graphene/carbon nanotubes, crystalline doping, and coatings for improving the electrochemical performance of these cathode materials.

**Keywords**
progress, design, strategies, research, synthesis, cathodes, performance, limn2o4

**Disciplines**
Engineering | Physical Sciences and Mathematics

**Publication Details**
Mao, F., Guo, W. & Ma, J. (2015). Research progress on design strategies, synthesis and performance of LiMn2O4-based cathodes. RSC Advances: an international journal to further the chemical sciences, 5 (127), 105248-105258.

RSC Advances

REVIEW

View Article Online
View Journal | View Issue



Cite this: *RSC Adv.*, 2015, **5**, 105248

# Research progress on design strategies, synthesis and performance of $LiMn_2O_4$-based cathodes

Fangxin Mao,[a] Wei Guo*[b] and Jianmin Ma*[ac]

Received 19th October 2015
Accepted 21st November 2015

DOI: 10.1039/c5ra21777f

www.rsc.org/advances

Spinel $LiMn_2O_4$ (LMO)-based composites, due to their combination of low toxicity, abundant natural resources, and excellent electrochemical performance, are regarded as promising candidate cathode materials for lithium ion batteries. Current energy storage demands are not being met with existing materials, however, because of their defects, such as fast capacity fading, low rate capability, and low specific capacity in practical applications. Manganese dissolution during electrochemical processes bears the major responsibility for capacity loss, apart from the electrolyte factor. Low electrical conductivity, low ionic diffusion efficiency, and large structural variation have adverse effects on the electrochemical performance of materials. With respect to these drawbacks, significant progress has been made recently on optimizing the performance of LMO-based cathode materials. In this work, we review recent progress in 1 structural design, designing composites with graphene/carbon nanotubes, crystalline doping, and coatings for improving the electrochemical performance of these cathode materials.

## 1 Introduction

As the supply of fossil fuels becomes deficient and aggravates global distribution, sustainable and clean energy is becoming more and more critical for supporting electric vehicles and other electronic devices. Energy storage is needed to take full advantage of renewable electricity generation (wind, wave and solar).[1] For energy storage, the lithium-ion secondary battery is the most promising device because of its high energy and power density, long cycle life, and high reliability, which are important considerations for the performance of electric vehicles and hybrid electric vehicles. In addition, its high gravimetric and volumetric energy densities provide advantages for digital electrical products, such as laptops, cell phones, and even microelectronic devices.[2,3]

Typically, a basic Li-ion battery consists of a cathode (positive electrode) and an anode (negative electrode), which are immersed in a specific electrolyte and isolated from each other with a separator. The lithium ions shuttle between the cathode and anode through the electrolyte and electrons move through the external circuit during the charging and discharging process, which is shown in Fig. 1 in a sketch of a classical commercial lithium ion cell from the 1970s, using $LiCoO_2$ and graphite as the cathode and anode, respectively. During the

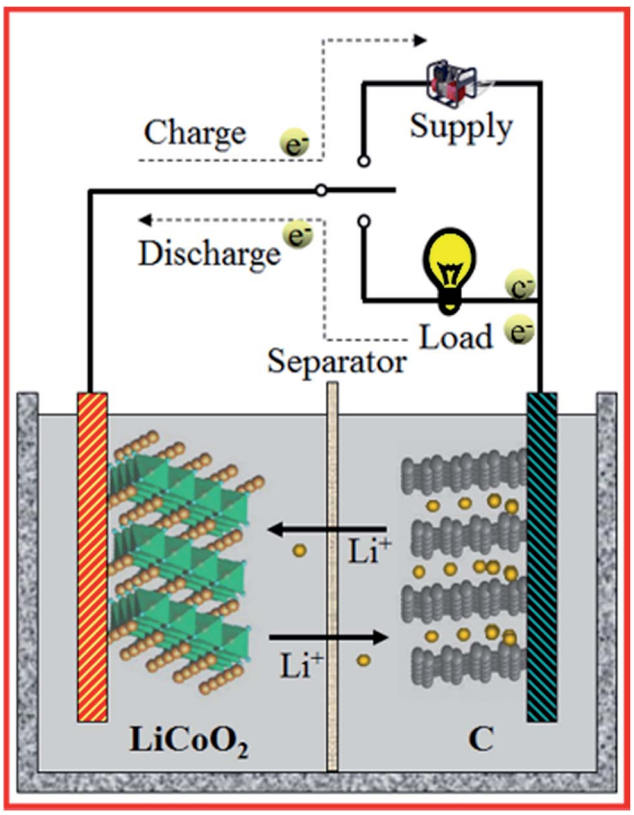


Fig. 1 Illustration to show the basic components and operation principle of a Li-ion cell. Reproduced with permission.[6]

[a]*Key Laboratory for Micro-/Nano-Optoelectronic Devices of the Ministry of Education, School of Physics and Electronics, Hunan University, Changsha 410082, P. R. China. E-mail: nanoelechem@hnu.edu.cn*

[b]*College of Chemistry and Chemical Engineering, Anyang Normal University, Anyang 455000, China. E-mail: wgnk@mail.nankai.edu.cn*

[c]*Institute for Superconducting and Electronic Materials, University of Wollongong, Wollongong 2500, Australia*

discharging process, the cathode accepts the electrons from the external load and lithium ions in the electrolyte. Conduction happens in two ways in the cycle circuit, *via* electrons and ion transfer. As it is known that the ionic mobility in an electrolyte is much smaller than the electrical conductivity in a metal, a cell needs a large contact surface between the electrodes and electrolyte. And a reversible loss of capacity occurs due to the limit of ionic diffusion while charging/discharging at a high rate is what leads to a loss of Li inserted into an electrode particle. However, in an electrochemical process, changes in electrode volume, electrode–electrolyte reaction, and/or electrode decomposition can cause an irreversible loss of capacity. The chemical reaction between an electrode and electrolyte results in the irreversible formation of a passivating solid-electrolyte interphase (SEI) layer when the initial charge of a cell is made in a discharge state.[4]

Although there has been research on Li-ion batteries for decades, there are many challenges involved to improve practical Li-ion secondary batteries, for example, improving their poor capacity and drastic capacity fading, which are keeping these batteries from meeting the ever-increasing demands for energy storage and limit their further spread to new applications. The properties of electrode active materials in the anode and cathode determine Li-ion battery performance to a large extent. Lithium manganese oxide-based materials have been attracting much attention as cathode materials because they have particular advantages, such as low cost, high potential platform, and high rate capability.[5]

The electrochemical reaction (intercalation/deintercalation of Li ions) that occurs in the $LiMn_2O_4$ cathode can be expressed as follows:

$$LiMn_2O_4 \leftrightarrow Li_{1-\delta}Mn_2O_4 + \delta Li^+ + \delta e^- \quad (1)$$

For this material, electrochemical intercalation/deintercalation of Li-ions occurs in the potential range of 3.0–4.5 V *vs.* lithium electrode, while reaction (1) occurs in two stages in the composite range of $0 \leq \delta \leq 0.5$ and $0.5 \leq \delta \leq 1$, and it has a theoretical specific capacity of 148 mA h $g^{-1}$.[7]

Lithium manganese oxide has a cubic spinel crystal structure, as shown in Fig. 2, in which oxygen ions occupy the 32e tetrahedral positions and exhibit dense cubic packing, manganese ions occupy the 16d octahedral positions, and the 8a tetrahedral positions are occupied by lithium ions. A site occupied by a lithium ion is separated from the four neighboring ions by voids at 16c, so three-dimensional (3-D) channels (8a–16c–8a–16c) provide a passage for potential migration of lithium ions in the crystal body.[7,8] In an insertion cathode, the 3-D passages provide a chance for high rate capability.[9] In addition, Kalantarian *et al.*[10] concluded that the $LiMn_2O_4$ crystal structure could be interpreted as that of an n- or p-type semiconductor during the delithiation or lithiation process, respectively, considering the density of states calculated by several density functional theory methods, suggesting that the structure could sustain high current rates. Yamada *et al.*[11] found that a $LiMn_2O_4$ thin film electrode requires less activation energy for transferring Li-ions, with a smaller increase after

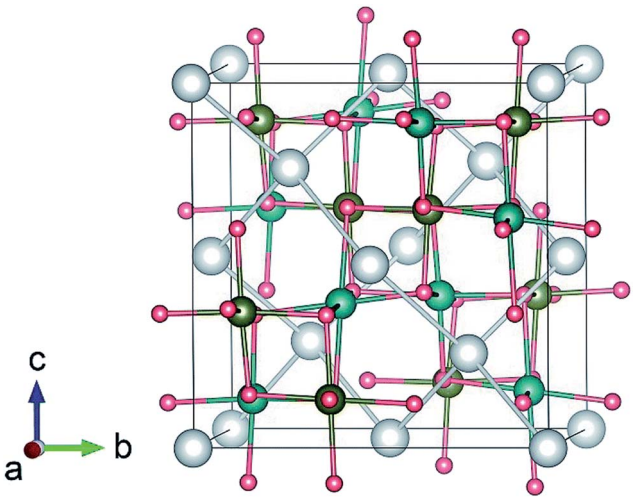


Fig. 2 Supercell model for spinel-type $LiMn_2O_4$ after structural optimization. Large gray spheres are Li, medium blue (yellow) spheres are $Mn^{3+}$ ($Mn^{4+}$), and small red spheres are O.[5] Copyright 2014, Royal Society of Chemistry.

cycling compared with the $LiCoO_2$ thin film electrode. During the delithiation or lithiation process, the composite can retain the stable structure of the spinel cubic. High voltage and tailoring of the potential window could be achieved, as has been reported in many papers, using $LiMn_2O_4$-based materials synthesized by a variety of methods.[12,13]

Despite the above-mentioned advantages, fast capacity fading during cycling at high temperature, which is due to such possible factors as manganese dissolution, and Jahn–Teller distortion, *etc.*, seriously limits such materials' practical life span.[14–17] As a semiconductor, $LiMn_2O_4$ has a band gap of 1.3 eV and low electrical conductivity ($\sim 10^{-6}$ S $cm^{-1}$), which leads to an inferior rate capability.[18] Some research has been done on the electrochemical behavior and degradation mechanism in Li-ion batteries. Tang *et al.*[19] investigated the electrochemical behavior and surface structure of $LiMn_2O_4$ when charged to high voltage, and found that drastic changes in the atomic-level structure occurred on the surface, in conjunction with faster manganese dissolution, which led to a degraded electrochemical performance. Lee *et al.*[20] utilized *in situ* transmission electron microscopy (TEM) technology to separately research the local phase transformations during the lithium-ion deintercalation process, and concluded that a cubic–tetragonal transition takes place during discharging, but not during the charging process, which is explained by the different diffusion rates of lithium ions between the surface and the bulk. The stability of the crystal phase determines the electrochemical performance of $LiMn_2O_4$ cathode materials to some extent. It is accepted by the majority of researchers that decreasing the Mn dissolution could alleviate the degradation of these cathode materials independently from the electrolyte content.[21] Elevated temperature will exacerbate the performance degeneration due to the enhancement of one or more circumstances of manganese dissolution, irreversible transition of the crystal phase and oxygen deficiency.[22] The capacity fade model for the spinel LMO

cathode built by Dai *et al.*[23] showed that 16% of the capacity degenerated after 50 cycles at C/3 and 55 °C between 3.5 and 4.5 V, which was approximate to the experimental result, and even more serious attenuation occurred at high rate cycles. Many factors lead to the fading of capacity, for example, the Li ion diffusion coefficient decreased from $3.5 \times 10^{-15}$ $m^2$ $s^{-1}$ to less than $2 \times 10^{-15}$ $m^2$ $s^{-1}$ ranging from the second cycle to the 50th cycle at 55 °C. Thus, increasing the resistance of Li ion migration in the surface films also accounted for the fading. It has become a brutal challenge to overcome the series of problems caused by high temperature.

Some important quantities should be endowed to an excellent cathode, such as high operating potential, fast electrochemical reaction kinetics with Li-ions and electrons, stable structure for fast delithiation or lithiation, short diffusion distance for electrons and Li-ions, high ionic diffusivity and electrical conductivity.[24] In addition, the thermostability of the materials should be noted to cope with various work circumstances caused by system thermogenesis. Through understanding the importance of the state of the crystal and surface, many reasonable strategies can be designed to improve the performance of the lithium manganese oxide cathode. In this paper, we review recent research progress on lithium manganese oxide-based cathode materials, with the focus on improving the cathode capacity and cycling performance through structural design, the use of composites with graphene/carbon nanotubes, crystalline doping, and coating methods.

## 2 Structural design

To enhance the battery performance, developing nanostructured electrode materials represents one of the most attractive strategies.[26] Islam and Fisher[27] have examined the fundamental features important to cathode performance, including voltage trends, ion diffusion paths and dimensions, intrinsic defect chemistry, and surface properties of nanostructures using computational techniques. And tuning the structure and properties of nanostructured cathode materials has been reported.[28] Shukla and Kumar[29] have summarized the use of nanoarchitectures, which could lead to improvements in terms of electrical and ionic conductivities, diffusion and mass transport, and electron transfer in electrochemical energy storage. It is generally recognized that a smaller particle size of the active material results in a shorter diffusion distance for lithium ions during electrochemical processes, which may be beneficial for battery performance. Smaller particles have greater structural integrity than bulk ones because of fewer pre-existing defects, as concluded by Raghavan *et al.*,[30] which is correlated with changes in the electrode particle surface area caused by particle fracture, and is related to solid electrolyte interphase (SEI) formation, isolation of the active material, and reduction in electrical conductivity. The structure or microstructure of the material grain can directly influence the properties of the electrode containing it.

Ragavendran *et al.*[31] demonstrated that nanoparticles derive their virtue of high rate capability not only from size effects, but also from the shape effect. Han *et al.*[32] synthesized single-phase, high-purity $LiMn_2O_4$ nanosized crystal powders as cathode materials for Li-ion batteries, and the results showed that a capacity of 116.6 mA h $g^{-1}$ was retained after 80 cycles. Cai *et al.*[33] reported $LiMn_2O_4$ octahedral nanoparticles with excellent cycling stability and rate capability (initial discharge capacity of 118.5 and 78.3 mA h $g^{-1}$, and about 72.49% and 94.6% of its initial discharge capacity could be retained, even after 1600 cycles at 10C and 3000 cycles at 20C, respectively). Octahedral and truncated octahedral spinel-type $LiMn_2O_4$ has been reported for cathode materials with excellent electrochemical performances.[33–36] One-dimensional nanofiber,[37–41] nanorod,[42–46] and nanowire[47,48] structures of spinel $LiMn_2O_4$ were studied in several papers. Aravindan *et al.*,[37] Kalluri *et al.*[38] and Kumar *et al.*[39] reported that electrospun nanofibers of $LiMn_2O_4$ had outstanding properties for lithium batteries. Recently, Zhou and co-workers[41] prepared an ultra-long spinel lithium manganese oxide nanofiber cathode *via* an electrospinning method, and the cathode materials showed a porous "network-like" morphology with nanosize diameters (~170 nm), microsize lengths, (~20 μm) and a pure spinel structure. Their discharge capacity was 146 mA h $g^{-1}$ at 0.1C; more importantly, the discharge capacities were 112 mA h $g^{-1}$, 103 mA h $g^{-1}$, and 92 mA h $g^{-1}$ at high discharge rates of 10C, 20C, and 30C, respectively. Xie and co-workers[46] applied a templating method to synthesize a single-crystalline spinel $LiMn_2O_4$ nanorod structure that exhibited a superior long cycle life, retaining 95.6% of the initial capacity after 1000 cycles at a 3C rate, with no deterioration of the morphology. Compared with the one-dimensional structure, spherical or anomalous nano/microscale pieces[49–56] are more prone to degradation and have bulk-like electrochemical performance due to their crystalline structure and size effectiveness. It should be noted that a porous cube structure as shown in Fig. 3[25] composed of single

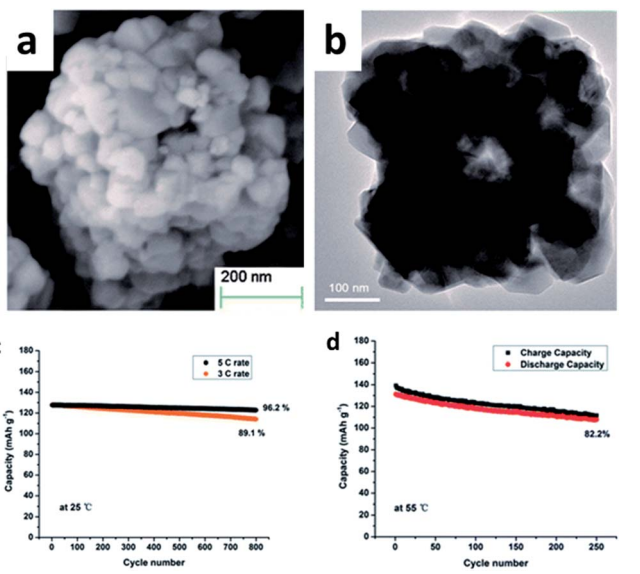


Fig. 3 Architecture of porous $LiMn_2O_4$ cubes: (a) SEM image, (b) TEM image, and the cycling performance of $LiMn_2O_4$ charged/discharged at rates of 3C and 5C at 25 °C (c) and at 5C at 55 °C (d) (1C = 148 mA $g^{-1}$).[25] Copyright 2014, Royal Society of Chemistry.

 

crystalline nanoparticles showed superior long-term cycling stability and high rate capability, delivering a reversible discharge capacity of 108 mA h $g^{-1}$ at a 30C rate and yielding a capacity retention of over 81% at a rate of 10C after 4000 cycles. Hierarchical porosity and structures are involved in newly developed materials for energy storage, which include the advantages of nanoparticles and eliminate their drawbacks to some degree.[57] Hierarchical $LiMn_2O_4$ microspheres,[58–60] nanofibers,[39] and doughnut-shaped[61] structures are common. A hierarchical $LiMn_2O_4$ phase with a layered nanostructure was also studied by Lee *et al.*, and it exhibited a high discharge capacity and excellent cycling stability at elevated temperature (60 °C).[62] Loading $LiMn_2O_4$ onto carbon fiber paper to create a binder-free positive electrode[63] and aligning multi-walled carbon nanotubes to form elastic and wearable wire-shaped lithium-ion batteries[64] are both creative examples of structures designed to improve the material's properties. Last, but not least, in a novel strategy, laser printing and femtosecond-laser structuring were applied in lithium-ion microbatteries, which optimized the cycling stability and capacity retention, and might enlighten researchers in the future.[65] As suggested above, the structure of materials plays an important role in electrochemical processes (Fig. 4).

## 3 Graphene/carbon nanotube composites

Graphene and carbon nanotubes (CNTs) are new types of promising materials and have become prime research topics. Here, we review their recent application in lithium manganese oxide cathodes. Graphene has been found to significantly improve cathode electrochemical performance in current studies, although it was previously applied as an electron-conducting additive for lithium ion cathode materials.[67] Sreelakshmi *et al.*[68] prepared the active materials in a graphene matrix for use in electrodes and obtained an enhanced energy and power density. Composites of nanocrystalline $LiMn_2O_4$ immobilized on the surface of graphene were developed using solvothermal[69] and hydrothermal[70] methods, and the nanocomposites showed a greatly improved electrochemical performance in terms of the specific capacity, cycling performance, and rate capability, which was attributable both to the improvement of the surface ion transport of nanocrystalline lithium manganate and to the increase in electrical conductivity. Ragavendran *et al.*[71] explained that graphene controlled crystal synthesis through its thermodynamic properties and this led to an orientation in the highly stable (400) direction, which offers superior electrochemical properties in general and much better rate capability in particular. Apart from graphene, one-dimensional carbon nanotubes (CNTs) have been used in cathode composites due to their unique properties. CNTs not only provide a conductive matrix, facilitating fast electron transport, but also effectively reduce agglomeration of the $LiMn_2O_4$ nanoparticles.[72] Guler *et al.*[73] investigated the effects of multiwall CNT (MWCNT) reinforcement on the electrochemical performance of $LiMn_2O_4$/MWCNT nanocomposite cathodes. The results showed that along with increasing MWCNT mass, from 0 wt% to 5.0 wt%, 10.0 wt%, and 15.0 wt%, there was capacity retention of 86.1, 129.4, 134.7, and 136.5 mA h $g^{-1}$, respectively, after 50 cycles. Higher electrical conductivity, higher structural stability of the composites, and rapid $Li^+$ diffusion, resulting from the open lattice channels and unique one-dimensional structure of the MWCNTs, could be major reasons for these changes. A high specific capacity of 145.4 mA h $g^{-1}$, close to the theoretical capacity of $LiMn_2O_4$ was achieved by a $LiMn_2O_4$/MWCNT nanocomposite, which also featured superior rate capability and cyclability.[74] A multiwall carbon nanotube network composite with $LiNi_{0.5}Mn_{1.5}O_4$ not only delivered 80% of the 1C capacity at 20C, but also featured a high working potential and very good cycling stability.[75] The same improvement effects were achieved by other researchers using a two-step hydrothermal approach (Fig. 5).[66,76]

## 4 Crystalline doping

Introducing a guest element into a LMO crystalline cell could affect the valence of Mn, the operating potential plot and the lattice of the crystal, all of which adjust the performance of the LMO cathode. In pure $LiMn_2O_4$, manganese ions can be partially replaced by other metal ions, and no damage to the spinel structure occurs, which was revealed by computational methods, but the electrical properties of the material are modified.[21] Single or multi-metal doping with metal ions, including Al, Ni, Co, Fe, Mg, Cu, V, Sm and Zn, was extensively

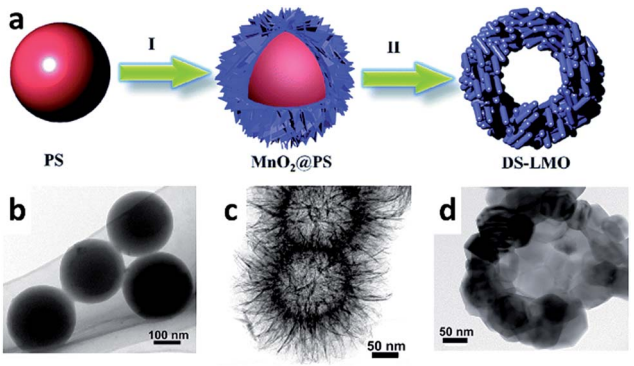


Fig. 4 (a) Schematic illustration of the synthesis procedure for doughnut-shaped $LiMn_2O_4$. TEM images of (b) PS spheres, (c) $MnO_2$@PS, and (d) DS-$LiMn_2O_4$.[61] Copyright 2015, Royal Society of Chemistry.

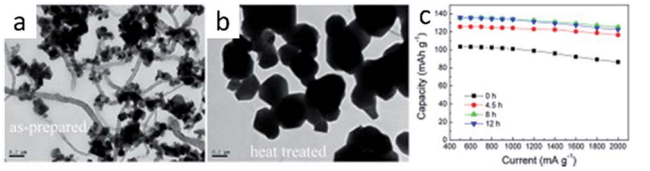


Fig. 5 TEM images of carbon nanotubes/$LiMn_2O_4$ after (a) hydrothermal processing and (b) heat-treatment. (c) Rate performance of CNT/LMO heat treated for different lengths of time.[66] Copyright 2013, Elsevier.

investigated for optimizing the electrochemical performance of Li-ion batteries, among which, Ni-doped $LiMn_2O_4$ has become one of the current research interests for a high potential cathode.[77–87] $LiNi_{0.5}Mn_{1.5}O_4$ is considered to be promising as a cathode material because of its excellent electrochemical performance with an operating voltage of 4.7 V and capacity of 135 mA h $g^{-1}$.[88–95] Hugues *et al.*[96] studied the relationship between the $Mn^{3+}$ content, structural ordering, phase transformation, and kinetic properties in $LiNi_xMn_{2-x}O_4$, and revealed that increasing the $Mn^{3+}$ content triggered the transition from ordered to disordered spinel, which led to increased solid solution behavior, reduced two-phase transformation domains, and improved transport properties during Li extraction and insertion. Further increasing the $Mn^{3+}$ content, however, in an already disordered structure extends the solid solution domain and eliminates the presence of phase II, so that it yields only a limited effect on rate capability. Shimoda *et al.*[97] used *in situ* and *ex situ* Li nuclear magnetic resonance (NMR) spectroscopy to study the delithiation/lithiation behavior of $LiNi_{0.5}Mn_{1.5}O_4$ and clarify the phase reactions during electrochemical processes. Wang *et al.*[98] reported the effect of oxygen deficiency on defect chemistry in delithiated spinel $LiNi_{0.5}Mn_{1.5}O_4$ cathodes, where the results revealed the progress of the atomic-level structural changes: oxygen deficiency promoted the migration of Ni and Mn ions, and the migration assisted the formation of oxygen vacancies. Luo *et al.*[99] reported high-voltage $LiNi_{0.5}Mn_{1.5}O_4$ hollow microspheres with high reversible capacities of 135.5, 147.5, and 132.1 mA h $g^{-1}$ at 0.1, 0.5, and 2C, respectively. Even at a high rate of 5C, the electrode retained 93.4% of the initial capacity at 0.1C. After investigating the improvement after Al doping, it was concluded by Guo *et al.*[100] that Al-doping facilitated rate and cycling capabilities at room and high temperature: the $LiAl_{0.1}Mn_{1.9}O_4$ sample was cycled at a rate of 5C, and the capacity retention ratio of the electrode after 100 cycles was about 95% at 25 °C and about 90% at 55 °C. Many researchers have shown that LMO-based cathode materials can be endowed with improved cycling stability and cycling performance at elevated temperatures through Al-doping methods.[101–106] LMO cathode materials doped with nanoparticles of the bimetallic metal alloys Au–Fe[107] and Pt–Au[108] were applied in lithium-ion batteries, which showed enhanced conduction and improved cyclability.

In addition to doping with transition metal cations, the semiconductor elements Si,[109,110] and Sb,[111] and non-metal anions, including $F^-$,[112,113] $Cl^-$,[114] $B^{3-}$,[115] and $PO_4^{3-}$,[116,117] were embedded into LMO crystals to change their attributes. Zhao *et al.*[109,110] researched low-level Si, Mg single and co-doping to improve the electrochemical performance of LMO cathode materials. Results showed that the cubic spinel structure of $LiMn_2O_4$ was preserved throughout the introduction of alien atoms. Equimolar $Mg^{2+}$ and $Si^{4+}$ ions could completely occupy the octahedral (16d) sites, replacing $Mn^{3+}$ and $Mn^{4+}$ ions, respectively, which significantly improved the structural stability and suppressed the Jahn–Teller distortion, so that a far higher reversible capacity was obtained. Cui *et al.* embedded Sb ions in a LMO crystal, and even though the impure phase of $LiSbO_3$ appeared, the composite featured higher cycling and rate capacities than the pure LMO material. In some ways, the introduction of Si and Sb led to positive effects. The halogen elements fluorine and chlorine could bond with manganese, forming electrovalent bonds that were stronger than Mn–O covalent bonds, so that substitution of stronger bonds for weaker ones led to a more stable structure.[114] The introduction of the trivalent anions $B^{3-}$ and $PO_4^{3-}$ led to increases in the *a* lattice parameter in both cases, without changing the spinel crystal structure, because their ionic radii were favorable for intercalation/deintercalation of Li-ions.

# 5 Surface coating

Two major activation processes, desolvation and lattice incorporation, were suggested for the Li-ion exchange reaction at the electrode/electrolyte interface.[118] Reactions and charge transfer at cathode–electrolyte interfaces affect the performance and the stability of Li-ion cells.[119] As it is well known that Mn dissolution is the major reason for capacity fading of the LMO-based cathode materials, formation of a stable solid electrolyte interface (SEI) film and protection of the integrity of the crystalline structure are effective in improving the electrochemical performance of electrode materials. Surface coating on active materials or the electrode could achieve this goal to some extent, because the outer layer forms a stable solid-electrolyte interphase that could protect Mn from dissolving into the electrolyte, protect the active materials from contact with HF acid, and improve the rate of lithium ion insertion and de-insertion. Wang *et al.*[120] summarized the application of surface and interface engineering in Li-ion batteries, and analyzed surface modifications from active surface and surface functionalization perspectives. Carbon (including organic compounds), lithium-metal–oxygen, metal oxides ($Al_2O_3$, $MnO_2$, $ZrO_2$, ZnO, $TiO_2$, *etc.*), fluorides ($AlF_3$, $FeF_3$, *etc.*), and some inorganic compounds were proposed and successfully applied to modify the surfaces of electrode materials. Considering that inorganic compounds are poor conductors, the noble metals Au[121] and Ag[122] were also used to modify the surfaces of active materials by some researchers, and they not only enhanced the conductivity, but also improved the cycle life. Meng *et al.*[123] reported that several of the materials mentioned above had been coated previously onto electrode materials to optimize lithium-ion batteries using the atomic layer deposition (ALD) method.

## 5.1 Carbon coating

Lee *et al.*[125] reported carbon-coated single-crystal $Li_2Mn_2O_4$ nanoparticle clusters with high gravimetric and volumetric energy and power density, which delivered 63% of the initial capacity after 2000 cycles at a charge/discharge rate of 20C. Coating with carbon may enhance the specific capacity apart from stabilizing the cycling performance. Noh *et al.* discovered that LMO with a thin graphitic layer doubled its capacity at a cut-off voltage of 2.5 V, which could be explained by the facile electron-transfer highways provided by the graphitic layer,

 

stabilizing the structural distortion due to the reaction in the 3 V region. A composite of LMO with a graphene-like carbon membrane coating synthesized by an *in situ* method reached 131.1 mA h $g^{-1}$ at room temperature, and up to 96% capacity was retained after 50 cycles at 0.1C.[126] Conductive polypyrrole (PPy)-coated $LiNi_{0.5}Mn_{1.5}O_4$ (LNMO)[127] showed remarkable stability, even at elevated temperature, and good voltage properties. Polypyrrole can increase the electrical conductivity and work as an effective protective layer to suppress the electrolyte decomposition arising from undesirable reactions between the cathode electrode and the electrolyte on the surface of the active material at elevated temperature. Sun *et al.*[124] reported that uniform carbon-coated spinel $LiMn_2O_4$ nanowires displayed an ultra-high rate and cycling performance, retaining 83% of the initial capacity after 1500 cycles, even at a rate of 30C. In addition to coating carbon materials directly onto active material particles, an electrode coating can also improve performance in Li-ion batteries. Sputtering a graphitic coating[128] and loading an ion exchange polymer coating[129] on the surfaces of cathodes have been studied, and enhanced performances were achieved (Fig. 6).

### 5.2 Metal oxide coating

Loïc *et al.*[131] studied the surface chemistry of metal-oxides (ZnO, $Al_2O_3$, and $ZrO_2$) coated on LNMO thin film cathodes *via* X-ray photoelectron spectroscopy (XPS) and found that ZnO decomposed during the first charge, whereas $Al_2O_3$ and $ZrO_2$ were stable for more than 100 cycles, which explains the poor cycle life of the ZnO coated cathode. $Al_2O_3$ and $ZrO_2$ coatings demonstrated good performance in other research.[132,133] Coating metal oxides with stable electrochemical properties onto the surface of active materials may yield a better improvement. Coatings of the manganese oxides $Mn_2O_3$,[134] $MnO_2$,[135,136] and MnO[137] were demonstrated as suitable ways to promote cycle life, due to decreased Mn dissolution after the coating process. $Y_2O_3$,[138] $V_2O_5$,[139] and $TiO_2$ (ref. 140) coatings all resulted in appreciable improvement of capacity and cycling stability at elevated temperature, and in addition, excellent rate capability was also found in the case of the former two. Composites with the multi-metal oxides In–Sn–O,[141] La–Sr–Mn–O,[142] and $La_{0.7}Sr_{0.3}Mn_{0.7}Co_{0.3}O_3$ (ref. 143) coated on LMO composites were also studied, among which, the last composite was also obviously enhanced, especially at high rates (10C, 20C, and 30C), in addition to having an excellent cycling stability. Michalska and Monika[144] modified the surface of LMO grains with $CeO_2$ by a low temperature method and obtained a super-stable cycling performance, with only 2% loss after 100 cycles at 1C. $RuO_2$ was applied to modify the surface of LNMO cathode materials, and a good cycling performance was the result: a specific capacity as high as 113.8 mA h $g^{-1}$ was preserved beyond 1000 cycles (Fig. 7).[130]

### 5.3 Lithium-metal–oxygen coating

Lu *et al.*[146] reported a surface-doping strategy, which combined the bulk-doping strategy and the surface-coating strategy, to yield a $TiO_2$-surface-doped $LiMn_2O_4$ material with a $LiMn_{2-x}Ti_xO_4$ layer on the outside of the particles. The same phenomenon occurs for the Al–Ga coating LMO spinel: the $LiMn_{2-x-y}Al_xGa_yO_4$ phase was formed on the outside, and an excellent electrochemical performance was obtained from −30 to 55 °C.[147] LMO spinel cathode materials coated with lithium-metal–oxygen have a more stable structure. This coating can enhance both the cycling stability, and the specific capacity. Pure spinel LMO with an epitaxial coating of a highly doped spinel has a hierarchical atomic structure consisting of a cubic spinel, tetragonal spinel, and layered structures, and can retain 90% of its capacity after 800 cycles at 60 °C.[148] Coating stoichiometric $LiMn_2O_4$ with a cobalt-substituted spinel results in good elevated temperature stability and rate capability.[149] The high voltage cathode material $LiNi_{0.5}Mn_{1.5}O_4$ was used to modify the surfaces of $Li_2Mn_2O_4$ cores, and good electrochemical performance was achieved.[150–153] $Li_2TiO_3$, $Li_{0.17}La_{0.61}TiO_3$, $Li_2ZrO_3$, $LiNbO_3$, and LiBO, *etc.* were researched with the aim of suppressing Mn dissolution and promoting good cell performance (Fig. 8).[145,154–159]

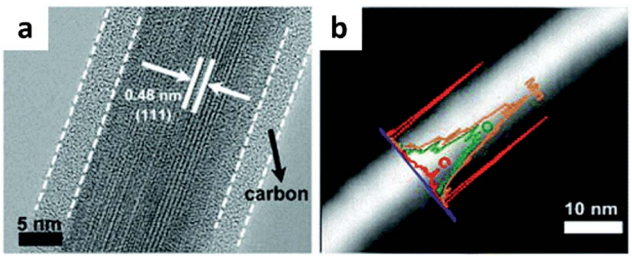


Fig. 6 HRTEM image (a) and dark-field STEM image (b) of a carbon-coated LMO nanowire.[124] Copyright 2015, Royal Society of Chemistry.

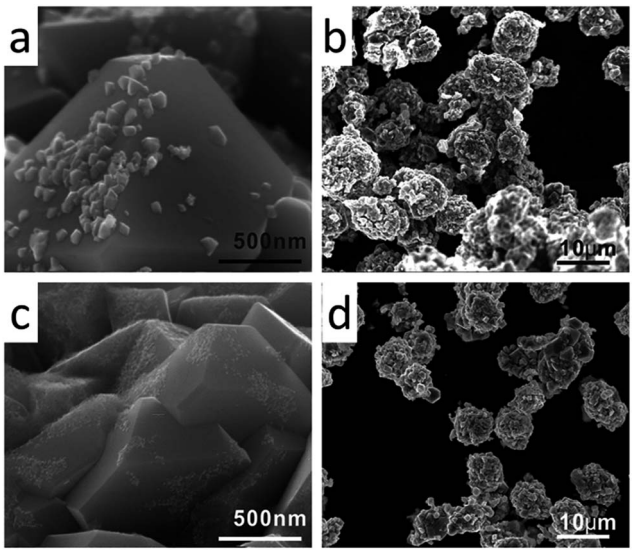


Fig. 7 SEM images of $RuO_2$-modified $LiNi_{0.5}Mn_{1.5}O_4$ (a and b); $Al_2O_3$ modified $LiNi_{0.5}Mn_{1.5}O_4$ (c and d).[130] Copyright 2015, Royal Society of Chemistry.

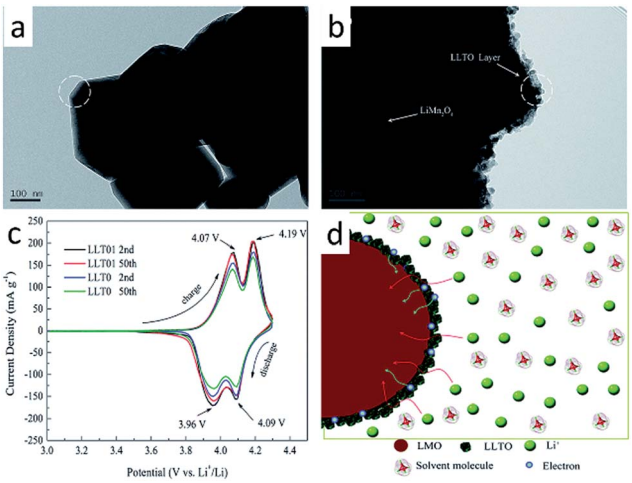


Fig. 8 (a and b) TEM images of $LiMn_2O_4$ with a $Li_{0.34}La_{0.51}TiO_3$ coating layer; (c) CV curves of the composites at a scan rate of 0.1 mV $s^{-1}$ after different cycles at a 1C rate at room temperature; (d) schematic illustration of the surface coating of a cathode.[145] Copyright 2015, Royal Society of Chemistry.

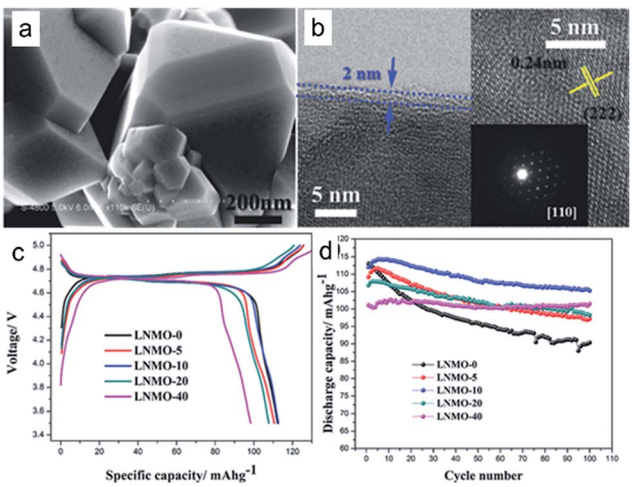


Fig. 9 (a) SEM and (b) TEM images of $LiNi_{0.5}Mn_{1.5}O_4$ with an active $FePO_4$ coating by atomic layer deposition, with the inset to (b) showing the corresponding electron diffraction pattern; (c) first charge/discharge curves and (d) cycling stability at 0.5C of samples with different coating times. Reproduced with permission.[160]

### 5.4 Fluoride/phosphate coatings

As identified by a number of researchers, HF acid attacks the active electrode materials and dissolves the transition metal cations in cells with a $LiPF_6$-based electrolyte, leading to solid deposits on the anode surface through the reduction reaction of the dissolved cations. Metal oxides on the cathode surface turn into metal fluorides, which are expected to be resistant to HF. Coating with fluorides inactive to HF provides an available method to protect active materials and decrease the interfacial charge transfer resistance.[120] Wu *et al.*[161] coated $MgF_2$ onto the $LiNi_{0.5}Mn_{1.5}O_4$ surface *via* a wet coating strategy and obtained an improved electrochemical performance. The Zhao research group studied $FeF_3$ (ref. 162) and $LaF_3$ (ref. 163) coated spinel $LiMn_2O_4$ and found that the cycling stabilities were enhanced at both room temperature (25 °C) and elevated temperature (55 °C) for both coatings. Phosphate ($MPO_4$) has been applied as a cathode for lithium-ion batteries and could provide continuous lithium insertion channels and considerable electrical conductivity. Xiao *et al.*[160] coated $LiNi_{0.5}Mn_{1.5}O_4$ with active $FePO_4$ by atomic layer deposition, and the results showed that the cycling stability and the conductivity increased with the coating mass, but there was a lower specific capacity. $Li_3PO_4$,[164] $YPO_4$ (ref. 165) and $SrHPO_4$ (ref. 166) coatings were found to improve the cycling stability and thermal stability in a LMO cathode (Fig. 9).

## 6 Conclusions

Spinel lithium-manganese-oxides are one of the most promising candidate cathode materials for Li-ion batteries with a high working potential and high rate performance. Many current challenges, related to cycling stability, thermal stability, rate capability, and specific capacity, have impeded further application in energy storage. Much work has been done and some achievements obtained towards the improvement of the electrochemical performance of LMO-based cathode materials. Several strategies, including structural design, the use of composites, and crystalline and surface engineering, have proven to be available ways to optimize their performance for Li-ion batteries.

To further develop $LiMn_2O_4$-based cathode materials, in addition to the strategies mentioned above, real reasons and mechanisms for material degradation during electrochemical processes should be explored clearly, and then better solutions can be studied. In addition: (i) new advanced materials, other than graphene and carbon nanotubes, applied to the $LiMn_2O_4$-based cathode should be an available breakthrough, (ii) new strategies for synthesizing $LiMn_2O_4$-based cathodes should be explored and (iii) $LiMn_2O_4$-based batteries can be improved through exploring novel electrolyte formulations.

## Acknowledgements

This work was supported by the National Natural Science Foundation of China (Grant No. 51302079). We also thank Dr Tania Silver from the Institute for Superconducting and Electronic Materials (University of Wollongong) for revising our manuscript.

## Notes and references

1 N.-S. Choi, Z. Chen, S. A. Freunberger, X. Ji, Y.-K. Sun, K. Amine, G. Yushin, L. F. Nazar, J. Cho and P. G. Bruce, *Angew. Chem., Int. Ed.*, 2012, **51**, 9994–10024.
2 Y. Wang, B. Liu, Q. Li, S. Cartmell, S. Ferrara, Z. D. Deng and J. Xiao, *J. Power Sources*, 2015, **286**, 330–345.
3 E. M. Erickson, C. Ghanty and D. Aurbach, *J. Phys. Chem. Lett.*, 2014, **5**, 3313–3324.

 

4 J. B. Goodenough and K.-S. Park, *J. Am. Chem. Soc.*, 2013, **135**, 1167–1176.
5 L. Ghadbeigi, J. K. Harada, B. R. Lettiere and T. D. Sparks, *Energy Environ. Sci.*, 2015, **8**, 1640–1650.
6 D. Deng, *Energy Sci. Eng.*, 2015, **3**, 385–418.
7 A. V. Potapenko and S. A. Kirillov, *J. Energy Chem.*, 2014, **23**, 543–558.
8 K. Hoang, *J. Mater. Chem. A*, 2014, **2**, 18271–18280.
9 M. Ø. Filsø, M. J. Turner, G. V. Gibbs, S. Adams, M. A. Spackman and B. B. Iversen, *Chem.–Eur. J.*, 2013, **19**, 15535–15544.
10 M. M. Kalantarian, S. Asgari and P. Mustarelli, *J. Mater. Chem. A*, 2014, **2**, 107–115.
11 I. Yamada, K. Miyazaki, T. Fukutsuka, Y. Iriyama, T. Abe and Z. Ogumi, *J. Power Sources*, 2015, **294**, 460–464.
12 A. Bhaskar, S. Krueger, V. Siozios, J. Li, S. Nowak and M. Winter, *Adv. Energy Mater.*, 2015, **5**, 1401156.
13 M. D. Levi, V. Dargel, Y. Shilina, V. Borgel, D. Aurbach and I. C. Halalay, *J. Power Sources*, 2015, **278**, 599–607.
14 Y. Kim, J. Lim and S. Kang, *Int. J. Quantum Chem.*, 2013, **113**, 148–154.
15 L. Cai, Y. Dai, M. Nicholson, R. E. White, K. Jagannathan and G. Bhatia, *J. Power Sources*, 2013, **221**, 191–200.
16 C.-H. Lu and S.-W. Lin, *J. Mater. Res.*, 2002, **17**, 1476–1481.
17 J. Darul, C. Lathe and P. Piszora, *RSC Adv.*, 2014, **4**, 65205–65212.
18 J. He, Y. Chen, P. Li, F. Fu, J. Liu and Z. Wang, *RSC Adv.*, 2015, **5**, 80063–80068.
19 D. Tang, L. Ben, Y. Sun, B. Chen, Z. Yang, L. Gu and X. Huang, *J. Mater. Chem. A*, 2014, **2**, 14519–14527.
20 S. Lee, Y. Oshima, E. Hosono, H. Zhou, K. Kim, H. M. Chang, R. Kanno and K. Takayanagi, *J. Phys. Chem. C*, 2013, **117**, 24236–24241.
21 A. Kraytsberg and Y. Ein-Eli, *Adv. Energy Mater.*, 2012, **2**, 922–939.
22 G. Xu, Z. Liu, C. Zhang, G. Cui and L. Chen, *J. Mater. Chem. A*, 2015, **3**, 4092–4123.
23 Y. Dai, L. Cai and R. E. White, *J. Electrochem. Soc.*, 2013, **160**, A182–A190.
24 Y. Tang, Y. Zhang, W. Li, B. Ma and X. Chen, *Chem. Soc. Rev.*, 2015, **44**, 5926–5940.
25 H. B. Lin, J. N. Hu, H. B. Rong, Y. M. Zhang, S. W. Mai, L. D. Xing, M. Q. Xu, X. P. Li and W. S. Li, *J. Mater. Chem. A*, 2014, **2**, 9272–9279.
26 H. Xia, Z. Luo and J. Xie, *Progress in Natural Science: Materials International*, 2012, **22**, 572–584.
27 M. S. Islam and C. A. J. Fisher, *Chem. Soc. Rev.*, 2014, **43**, 185–204.
28 G.-L. Xu, Q. Wang, J.-C. Fang, Y.-F. Xu, J.-T. Li, L. Huang and S.-G. Sun, *J. Mater. Chem. A*, 2014, **2**, 19941–19962.
29 A. K. Shukla and T. Prem Kumar, *Wiley Interdiscip. Rev.: Energy Environ.*, 2013, **2**, 14–30.
30 R. S. Raghavan, A. M. Kumar and R. Narayanrao, *Z. Angew. Math. Mech.*, 2014, 1–14.
31 K. R. Ragavendran, H. Xia, G. Yang, D. Vasudevan, B. Emmanuel, D. Sherwood and A. K. Arof, *Phys. Chem. Chem. Phys.*, 2014, **16**, 2553–2560.
32 C.-G. Han, C. Zhu, G. Saito and T. Akiyama, *Adv. Powder Technol.*, 2015, **26**, 665–671.
33 Y. Cai, Y. Huang, X. Wang, D. Jia, W. Pang, Z. Guo, Y. Du and X. Tang, *J. Power Sources*, 2015, **278**, 574–581.
34 B.-M. Hwang, S.-J. Kim, Y.-W. Lee, H.-C. Park, D.-M. Kim and K.-W. Park, *Mater. Chem. Phys.*, 2015, **158**, 138–143.
35 S. Huang, H. Wu, P. Chen, Y. Guo, B. Nie, B. Chen, H. Liu and Y. Zhang, *J. Mater. Chem. A*, 2015, **3**, 3633–3640.
36 G. Jin, H. Qiao, H. Xie, H. Wang, K. He, P. Liu, J. Chen, Y. Tang, S. Liu and C. Huang, *Electrochim. Acta*, 2014, **150**, 1–7.
37 V. Aravindan, J. Sundaramurthy, P. S. Kumar, N. Shubha, W. C. Ling, S. Ramakrishna and S. Madhavi, *Nanoscale*, 2013, **5**, 10636–10645.
38 S. Kalluri, K. H. Seng, Z. Guo, H. K. Liu and S. X. Dou, *RSC Adv.*, 2013, **3**, 25576–25601.
39 P. S. Kumar, J. Sundaramurthy, S. Sundarrajan, V. J. Babu, G. Singh, S. I. Allakhverdiev and S. Ramakrishna, *Energy Environ. Sci.*, 2014, **7**, 3192–3222.
40 M. Qian, J. Huang, S. Han and X. Cai, *Electrochim. Acta*, 2014, **120**, 16–22.
41 H. Zhou, X. Ding, G. Liu, Y. Jiang, Z. Yin and X. Wang, *Electrochim. Acta*, 2015, **152**, 274–279.
42 Z. Li, L. Wang, K. Li and D. Xue, *J. Alloys Compd.*, 2013, **580**, 592–597.
43 D. Zhan, Q. Zhang, X. Hu, G. Zhu and T. Peng, *Solid State Ionics*, 2013, **239**, 8–14.
44 D. Zhan, F. Yang, Q. Zhang, X. Hu and T. Peng, *Electrochim. Acta*, 2014, **129**, 364–372.
45 H. Zhao, F. Li, X. Liu, W. Xiong, B. Chen, H. Shao, D. Que, Z. Zhang and Y. Wu, *Electrochim. Acta*, 2015, **166**, 124–133.
46 X. Xie, D. Su, B. Sun, J. Zhang, C. Wang and G. Wang, *Chem.–Eur. J.*, 2014, **20**, 17125–17131.
47 L. Mai, X. Tian, X. Xu, L. Chang and L. Xu, *Chem. Rev.*, 2014, **114**, 11828–11862.
48 Y. Wang, Y. Wang, D. Jia, Z. Peng, Y. Xia and G. Zheng, *Nano Lett.*, 2014, **14**, 1080–1084.
49 D. Guo, Z. Chang, B. Li, H. Tang, X.-Z. Yuan and H. Wang, *Solid State Ionics*, 2013, **237**, 34–39.
50 J. Jiang, K. Du, Y. Cao, Z. Peng, G. Hu and J. Duan, *J. Alloys Compd.*, 2013, **577**, 138–142.
51 Q. Jiang, X. Wang, C. Miao and Z. Tang, *RSC Adv.*, 2013, **3**, 12088–12090.
52 Y. Wang, X. Shao, H. Xu, M. Xie, S. Deng, H. Wang, J. Liu and H. Yan, *J. Power Sources*, 2013, **226**, 140–148.
53 Z. Yang, Y. Jiang, H.-H. Xu and Y.-H. Huang, *Electrochim. Acta*, 2013, **106**, 63–68.
54 D. Guo, Z. Chang, H. Tang, B. Li, X. Xu, X.-Z. Yuan and H. Wang, *Electrochim. Acta*, 2014, **123**, 254–259.
55 Y. Mizuno, N. Zettsu, H. Inagaki, S. Komine, K. Kami, K. Yubuta, H. Wagata, S. Oishi and K. Teshima, *CrystEngComm*, 2014, **16**, 1157–1162.
56 D. Guo, X. Wei, Z. Chang, H. Tang, B. Li, E. Shangguan, K. Chang, X.-Z. Yuan and H. Wang, *J. Alloys Compd.*, 2015, **632**, 222–228.
57 Y. Li, Z.-Y. Fu and B.-L. Su, *Adv. Funct. Mater.*, 2012, **22**, 4634–4667.

58 Y. Gu, Z. Tang, Y. Deng and L. Wang, *Electrochim. Acta*, 2013, **94**, 165–171.
59 H. Zhang, Y. Xu and D. Liu, *RSC Adv.*, 2015, **5**, 11091–11095.
60 L. Xiao, Y. Guo, D. Qu, B. Deng, H. Liu and D. Tang, *J. Power Sources*, 2013, **225**, 286–292.
61 W. Sun, H. Liu, T. Peng, Y. Liu, G. Bai, S. Kong, S. Guo, M. Li and X.-Z. Zhao, *J. Mater. Chem. A*, 2015, **3**, 8165–8170.
62 M.-J. Lee, S. Lee, P. Oh, Y. Kim and J. Cho, *Nano Lett.*, 2014, **14**, 993–999.
63 G. H. Waller, S. Y. Lai, B. H. Rainwater and M. Liu, *J. Power Sources*, 2014, **251**, 411–416.
64 J. Ren, Y. Zhang, W. Bai, X. Chen, Z. Zhang, X. Fang, W. Weng, Y. Wang and H. Peng, *Angew. Chem.*, 2014, **126**, 7998–8003.
65 J. Pröll, H. Kim, A. Piqué, H. J. Seifert and W. Pfleging, *J. Power Sources*, 2014, **255**, 116–124.
66 M. Tang, A. Yuan, H. Zhao and J. Xu, *J. Power Sources*, 2013, **235**, 5–13.
67 G. Kucinskis, G. Bajars and J. Kleperis, *J. Power Sources*, 2013, **240**, 66–79.
68 K. V. Sreelakshmi, S. Sasi, A. Balakrishnan, N. Sivakumar, A. S. Nair, S. V. Nair and K. R. V. Subramanian, *Energy Technol.*, 2014, **2**, 257–262.
69 K.-Y. Jo, S.-Y. Han, J. M. Lee, I. Y. Kim, S. Nahm, J.-W. Choi and S.-J. Hwang, *Electrochim. Acta*, 2013, **92**, 188–196.
70 B. Lin, Q. Yin, H. Hu, F. Lu and H. Xia, *J. Solid State Chem.*, 2014, **209**, 23–28.
71 K. Ragavendran, X. Hui, X. Gu, D. Sherwood, B. Emmanuel and A. K. Arof, *RSC Adv.*, 2014, **4**, 60106–60111.
72 H. Xia, K. R. Ragavendran, J. Xie and L. Lu, *J. Power Sources*, 2012, **212**, 28–34.
73 M. O. Guler, A. Akbulut, T. Cetinkaya and H. Akbulut, *Int. J. Energy Res.*, 2014, **38**, 509–517.
74 M. Tang, A. Yuan and J. Xu, *Electrochim. Acta*, 2015, **166**, 244–252.
75 X. Fang, C. Shen, M. Ge, J. Rong, Y. Liu, A. Zhang, F. Wei and C. Zhou, *Nano Energy*, 2015, **12**, 43–51.
76 B.-K. Zou, X.-H. Ma, Z.-F. Tang, C.-X. Ding, Z.-Y. Wen and C.-H. Chen, *J. Power Sources*, 2014, **268**, 491–497.
77 J. Liu, W. Liu, S. Ji, Y. Zhou, P. Hodgson and Y. Li, *ChemPlusChem*, 2013, **78**, 636–641.
78 M. Prabu, M. V. Reddy, S. Selvasekarapandian, G. V. Subba Rao and B. V. R. Chowdari, *Electrochim. Acta*, 2013, **88**, 745–755.
79 K. Dai, J. Mao, Z. Li, Y. Zhai, Z. Wang, X. Song, V. Battaglia and G. Liu, *J. Power Sources*, 2014, **248**, 22–27.
80 B. Ebin, S. Gürmen and G. Lindbergh, *Ceram. Int.*, 2014, **40**, 1019–1027.
81 M. Xiang, C.-W. Su, L. Feng, M. Yuan and J. Guo, *Electrochim. Acta*, 2014, **125**, 524–529.
82 M. Yavuz, N. Kiziltas-Yavuz, A. Bhaskar, M. Scheuermann, S. Indris, F. Fauth, M. Knapp and H. Ehrenberg, *Z. Anorg. Allg. Chem.*, 2014, **640**, 3118–3126.
83 D.-L. Fang, J.-C. Li, X. Liu, P.-F. Huang, T.-R. Xu, M.-C. Qian and C.-H. Zheng, *J. Alloys Compd.*, 2015, **640**, 82–89.
84 Y. Shi, S. Zhu, C. Zhu, Y. Li, Z. Chen and D. Zhang, *Electrochim. Acta*, 2015, **154**, 17–23.
85 R. Thirunakaran, R. Ravikumar, S. Gopukumar and A. Sivashanmugam, *J. Alloys Compd.*, 2013, **556**, 266–273.
86 M. C. Kim, K.-W. Nam, E. Hu, X.-Q. Yang, H. Kim, K. Kang, V. Aravindan, W.-S. Kim and Y.-S. Lee, *ChemSusChem*, 2014, **7**, 829–834.
87 A. M. Khedr, M. M. Abou-Sekkina and F. G. El-Metwaly, *J. Electron. Mater.*, 2013, **42**, 1275–1281.
88 Z. Lu, X. Rui, H. Tan, W. Zhang, H. H. Hng and Q. Yan, *ChemPlusChem*, 2013, **78**, 218–221.
89 Z. Chen, R. Zhao, P. Du, H. Hu, T. Wang, L. Zhu and H. Chen, *J. Mater. Chem. A*, 2014, **2**, 12835–12848.
90 J.-H. Kim, N. P. W. Pieczonka and L. Yang, *ChemPhysChem*, 2014, **15**, 1940–1954.
91 D. Liu, W. Zhu, J. Trottier, C. Gagnon, F. Barray, A. Guerfi, A. Mauger, H. Groult, C. M. Julien, J. B. Goodenough and K. Zaghib, *RSC Adv.*, 2014, **4**, 154–167.
92 A. Manthiram, K. Chemelewski and E.-S. Lee, *Energy Environ. Sci.*, 2014, **7**, 1339–1350.
93 H. Liu, G. Zhu, L. Zhang, Q. Qu, M. Shen and H. Zheng, *J. Power Sources*, 2015, **274**, 1180–1187.
94 X. Feng, Y. Tian, J. Zhang and L. Yin, *Powder Technol.*, 2014, **253**, 35–40.
95 S. Yang, J. Chen, Y. Liu and B. Yi, *J. Mater. Chem. A*, 2014, **2**, 9322–9330.
96 H. Duncan, B. Hai, M. Leskes, C. P. Grey and G. Chen, *Chem. Mater.*, 2014, **26**, 5374–5382.
97 K. Shimoda, M. Murakami, H. Komatsu, H. Arai, Y. Uchimoto and Z. Ogumi, *J. Phys. Chem. C*, 2015, **119**, 13472–13480.
98 Z. Wang, Q. Su, H. Deng and Y. Fu, *ChemElectroChem*, 2015, **2**, 1182–1186.
99 H. Luo, P. Nie, L. Shen, H. Li, H. Deng, Y. Zhu and X. Zhang, *ChemElectroChem*, 2015, **2**, 127–133.
100 D. Guo, B. Li, Z. Chang, H. Tang, X. Xu, K. Chang, E. Shangguan, X.-Z. Yuan and H. Wang, *Electrochim. Acta*, 2014, **134**, 338–346.
101 M. A. Kebede, M. J. Phasha, N. Kunjuzwa, L. J. le Roux, D. Mkhonto, K. I. Ozoemena and M. K. Mathe, *Sustainable Energy Technologies and Assessments*, 2014, **5**, 44–49.
102 X. Yi, X. Wang, B. Ju, Q. Wei, X. Yang, G. Zou, H. Shu and L. Hu, *J. Alloys Compd.*, 2014, **604**, 50–56.
103 F.-D. Yu, Z.-B. Wang, F. Chen, J. Wu, X.-G. Zhang and D.-M. Gu, *J. Power Sources*, 2014, **262**, 104–111.
104 X. Ding, H. Zhou, G. Liu, Z. Yin, Y. Jiang and X. Wang, *J. Alloys Compd.*, 2015, **632**, 147–151.
105 Y. Fu, H. Jiang, Y. Hu, Y. Dai, L. Zhang and C. Li, *Ind. Eng. Chem. Res.*, 2015, **54**, 3800–3805.
106 F. P. Nkosi, C. J. Jafta, M. Kebede, L. le Roux, M. K. Mathe and K. I. Ozoemena, *RSC Adv.*, 2015, **5**, 32256–32262.
107 N. West, K. I. Ozoemena, C. O. Ikpo, P. G. L. Baker and E. I. Iwuoha, *Electrochim. Acta*, 2013, **101**, 86–92.
108 N. Ross, E. I. Iwuoha, C. O. Ikpo, P. Baker, N. Njomo, S. N. Mailu, M. Masikini, N. Matinise, A. Tsegaye, N. Mayedwa, T. Waryo, K. I. Ozoemena and A. Williams, *Electrochim. Acta*, 2014, **128**, 178–183.

 

109 H. Zhao, F. Li, X. Liu, C. Cheng, Z. Zhang, Y. Wu, W. Xiong and B. Chen, *Electrochim. Acta*, 2015, **151**, 263–269.
110 H. Zhao, X. Liu, C. Cheng, Q. Li, Z. Zhang, Y. Wu, B. Chen and W. Xiong, *J. Power Sources*, 2015, **282**, 118–128.
111 P. Cui, Y. Liang, D. Zhan, Y. Zhao and R. Peng, *RSC Adv.*, 2014, **4**, 43821–43827.
112 H. R. Lee, B. Lee, K. Y. Chung, B. W. Cho, K.-Y. Lee and S. H. Oh, *Electrochim. Acta*, 2014, **136**, 396–403.
113 H. Li, Y. Luo, J. Xie, Q. Zhang and L. Yan, *J. Alloys Compd.*, 2015, **639**, 346–351.
114 D.-W. Han, W.-H. Ryu, W.-K. Kim, J.-Y. Eom and H.-S. Kwon, *J. Phys. Chem. C*, 2013, **117**, 4913–4919.
115 B. Ebin, G. Lindbergh and S. Gürmen, *J. Alloys Compd.*, 2015, **620**, 399–406.
116 R. A. Rodríguez, Y. M. Laffita, E. P. Cappe, M. A. A. Frutis, J. S. Salazar and O. L. Alves, *Ceram. Int.*, 2014, **40**, 12413–12422.
117 J. Kang, J. Song, S. Kim, J. Gim, J. Jo, V. Mathew, J. Han and J. Kim, *RSC Adv.*, 2013, **3**, 25640–25643.
118 M. Nakayama, H. Taki, T. Nakamura, S. Tokuda, R. Jalem and T. Kasuga, *J. Phys. Chem. C*, 2014, **118**, 27245–27251.
119 R. Hausbrand, D. Becker and W. Jaegermann, *Prog. Solid State Chem.*, 2014, **42**, 175–183.
120 K. X. Wang, X. H. Li and J. S. Chen, *Adv. Mater.*, 2015, **27**, 527–545.
121 J. L. Esbenshade, M. D. Fox and A. A. Gewirth, *J. Electrochem. Soc.*, 2015, **162**, A26–A29.
122 R. Jiang, C. Cui, H. Ma, H. Ma and T. Chen, *J. Electroanal. Chem.*, 2015, **744**, 69–76.
123 X. Meng, X.-Q. Yang and X. Sun, *Adv. Mater.*, 2012, **24**, 3589–3615.
124 W. Sun, H. Liu, Y. Liu, G. Bai, W. Liu, S. Guo and X. Zhao, *Nanoscale*, 2015, **7**, 13173–13180.
125 S. Lee, Y. Cho, H.-K. Song, K. T. Lee and J. Cho, *Angew. Chem.*, 2012, **124**, 8878–8882.
126 H. Zhuo, S. Wan, C. He, Q. Zhang, C. Li, D. Gui, C. Zhu, H. Niu and J. Liu, *J. Power Sources*, 2014, **247**, 721–728.
127 X.-W. Gao, Y.-F. Deng, D. Wexler, G.-H. Chen, S.-L. Chou, H.-K. Liu, Z.-C. Shi and J.-Z. Wang, *J. Mater. Chem. A*, 2015, **3**, 404–411.
128 J. Wang, Q. Zhang, X. Li, Z. Wang, H. Guo, D. Xu and K. Zhang, *Phys. Chem. Chem. Phys.*, 2014, **16**, 16021–16029.
129 P. Xue, D. Gao, S. Chen, S. Zhao, B. Wang and L. Li, *RSC Adv.*, 2014, **4**, 52624–52628.
130 D. Hong, Y. Guo, H. Wang, J. Zhou and H.-T. Fang, *J. Mater. Chem. A*, 2015, **3**, 15457–15465.
131 L. Baggetto, N. J. Dudney and G. M. Veith, *Electrochim. Acta*, 2013, **90**, 135–147.
132 J. Zhao and Y. Wang, *Nano Energy*, 2013, **2**, 882–889.
133 X. Fang, M. Ge, J. Rong, Y. Che, N. Aroonyadet, X. Wang, Y. Liu, A. Zhang and C. Zhou, *Energy Technol.*, 2014, **2**, 159–165.
134 J. H. Lee and K. J. Kim, *Electrochim. Acta*, 2013, **102**, 196–201.
135 B. J. Kang, J.-B. Joo, J. K. Lee and W. Choi, *J. Electroanal. Chem.*, 2014, **728**, 34–40.
136 L. Li, W. Qu, F. Liu, T. Zhao, X. Zhang, R. Chen and F. Wu, *Appl. Surf. Sci.*, 2014, **315**, 59–65.
137 J. Zeng, M. Li, X. Li, C. Chen, D. Xiong, L. Dong, D. Li, A. Lushington and X. Sun, *Appl. Surf. Sci.*, 2014, **317**, 884–891.
138 B. Ju, X. Wang, C. Wu, X. Yang, H. Shu, Y. Bai, W. Wen and X. Yi, *J. Alloys Compd.*, 2014, **584**, 454–460.
139 J. Wang, S. Yao, W. Lin, B. Wu, X. He, J. Li and J. Zhao, *J. Power Sources*, 2015, **280**, 114–124.
140 Y. Shang, X. Lin, X. Lu, T. Huang and A. Yu, *Electrochim. Acta*, 2015, **156**, 121–126.
141 C.-S. Kim, S.-H. Kwon and J.-W. Yoon, *J. Alloys Compd.*, 2014, **586**, 574–580.
142 H.-Q. Wang, F.-Y. Lai, Y. Li, X.-H. Zhang, Y.-G. Huang, S.-J. Hu and Q.-Y. Li, *Electrochim. Acta*, 2015, **177**, 290–297.
143 T. Shi, Y. Dong, C.-M. Wang, F. Tao and L. Chen, *J. Power Sources*, 2015, **273**, 959–965.
144 M. Michalska, B. Hamankiewicz, D. Ziółkowska, M. Krajewski, L. Lipińska, M. Andrzejczuk and A. Czerwiński, *Electrochim. Acta*, 2014, **136**, 286–291.
145 S. Hu, Y. Li, F. Lai, X. Zhang, Q. Li, Y. Huang, X. Yuan, J. Chen and H. Wang, *RSC Adv.*, 2015, **5**, 17592–17600.
146 J. Lu, C. Zhan, T. Wu, J. Wen, Y. Lei, A. J. Kropf, H. Wu, D. J. Miller, J. W. Elam, Y.-K. Sun, X. Qiu and K. Amine, *Nat. Commun.*, 2014, **5**, 5693.
147 F.-Y. Hung and K.-Y. Yang, *J. Power Sources*, 2014, **268**, 7–13.
148 S. Lee, G. Yoon, M. Jeong, M.-J. Lee, K. Kang and J. Cho, *Angew. Chem.*, 2015, **127**, 1169–1174.
149 M. Jeong, M.-J. Lee, J. Cho and S. Lee, *Adv. Energy Mater.*, 2015, 1500440–1500447.
150 Z. Han, X. Jia, H. Zhan and Y. Zhou, *Electrochim. Acta*, 2013, **114**, 772–778.
151 Y. Chae, J. K. Lee and W. Choi, *J. Electroanal. Chem.*, 2014, **730**, 20–25.
152 W. Liu, J. Liu, K. Chen, S. Ji, Y. Wan, Y. Zhou, D. Xue, P. Hodgson and Y. Li, *Chem.–Eur. J.*, 2014, **20**, 824–830.
153 T. Qiu, J. Wang, Y. Lu and W. Yang, *Electrochim. Acta*, 2014, **147**, 626–635.
154 H. Deng, P. Nie, H. Luo, Y. Zhang, J. Wang and X. Zhang, *J. Mater. Chem. A*, 2014, **2**, 18256–18262.
155 S. Kim, M. Hirayama, K. Suzuki and R. Kanno, *Solid State Ionics*, 2014, **262**, 578–581.
156 X. Yi, X. Wang, B. Ju, H. Shu, W. Wen, R. Yu, D. Wang and X. Yang, *Electrochim. Acta*, 2014, **134**, 143–149.
157 Z.-J. Zhang, S.-L. Chou, Q.-F. Gu, H.-K. Liu, H.-J. Li, K. Ozawa and J.-Z. Wang, *ACS Appl. Mater. Interfaces*, 2014, **6**, 22155–22165.
158 C. Du, M. Yang, J. Liu, S. Sun, Z. Tang, D. Qu and X. Zhang, *RSC Adv.*, 2015, **5**, 57293–57299.
159 J.-H. Kim, N. P. W. Pieczonka, P. Lu, Z. Liu, R. Qiao, W. Yang, M. M. Tessema, Y.-K. Sun and B. R. Powell, *ACS Appl. Mater. Interfaces*, 2015, **2**, 1500109–1500122.
160 B. Xiao, J. Liu, Q. Sun, B. Wang, M. N. Banis, D. Zhao, Z. Wang, R. Li, X. Cui, T.-K. Sham and X. Sun, *Adv. Sci.*, 2015, **2**, 1500022–1500028.
161 Q. Wu, X. Zhang, S. Sun, N. Wan, D. Pan, Y. Bai, H. Zhu, Y.-S. Hu and S. Dai, *Nanoscale*, 2015, **7**, 15609–15617.

162 S. Zhao, Y. Bai, Q. Chang, Y. Yang and W. Zhang, *Electrochim. Acta*, 2013, **108**, 727–735.
163 S. Zhao, Q. Chang, K. Jiang, Y. Bai, Y. Yang and W. Zhang, *Solid State Ionics*, 2013, **253**, 1–7.
164 J. Chong, S. Xun, J. Zhang, X. Song, H. Xie, V. Battaglia and R. Wang, *Chem.–Eur. J.*, 2014, **20**, 7479–7485.
165 S. Zhao, Y. Bai, L. Ding, B. Wang and W. Zhang, *Solid State Ionics*, 2013, **247–248**, 22–29.
166 X. Zhang, Y. Xu, H. Zhang, C. Zhao and X. Qian, *Electrochim. Acta*, 2014, **145**, 201–208.